

AD-A132 364

MEASUREMENT OF FRICTION AND WEAR ON MODIFIED SURFACES
(U) GEO-CENTERS INC NEWTON UPPER FALLS MA AUG 83
GC-TR-83-286 N00014-82-C-2092

1/

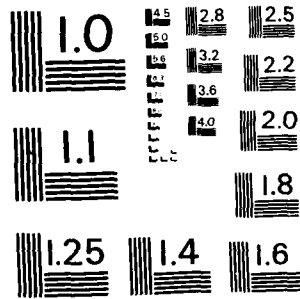
UNCLASSIFIED

F/G 11/6

NL



END
DATE
FILMED
9 83



MICROCOPY RESOLUTION TEST CHART
NATIONAL BUREAU OF STANDARDS-1963-A

12

ADA 132364

L

GC-TR-83-286

MEASUREMENT OF FRICTION AND WEAR
ON MODIFIED SURFACES

DTIC FILE COPY

DTIC
ELECTE
SEP 13 1983
S D
D

GEO-CENTERS, INC.

DISTRIBUTION STATEMENT A
Approved for public release;
Distribution Unlimited

83 08 15 007

Accession For	
NTIS GRA&I	<input checked="" type="checkbox"/>
DTIC TAB	<input type="checkbox"/>
Unannounced	<input type="checkbox"/>
Justification	
By	
Distribution/	
Availability Codes	
Dist	Avail and/or Special
A	



GC-TR-83-286

MEASUREMENT OF FRICTION AND WEAR
ON MODIFIED SURFACES

PREPARED FOR
U.S. NAVAL RESEARCH LABORATORY
4555 OVERLOOK AVENUE
WASHINGTON, D.C.
CONTRACT NUMBER N00014-82-C-2092

PREPARED BY
GEO-CENTERS, INC.
320 NEEDHAM STREET
NEWTON UPPER FALLS, MA 02164

AUGUST 1983

DISTRIBUTION STATEMENT A
Approved for public release
Distribution Unlimited

GEO-CENTERS, INC.

TABLE OF CONTENTS

	<u>Page</u>
Acknowledgments	ii
Measurement of Friction and Wear on Modified Surfaces . .	1
Table 1	7
Table 2	8
Figure 1	9
References	10

ACKNOWLEDGMENTS

We thank the Surface Modification and Analyses Branch of the U.S. Naval Research Laboratory for their support and cooperation with implantation.

MEASUREMENT OF FRICTION AND WEAR ON MODIFIED SURFACES

Dry sliding friction and wear measurements were used to evaluate two implantation processes which increase the C concentration in Ti-implanted steels. In one process, C is implanted into a Ti-implanted steel; in the second Ti is implanted at a lower energy to enhance the efficiency of the vacuum carburization process. Auger spectroscopy and energy-dispersive X-ray analyses were used to analyze the compositions produced by the implantation processes. The low energy (50 keV/ion) Ti-implantation process produced a low friction ($\mu=0.3$), wear resistant surface at a lower fluence ($2 \times 10^{17}/\text{cm}^2$) than the dual (C+Ti) implantation process at 50 keV/C ion and 190 keV/Ti ion, respectively. The 50 keV Ti-implantation produced more carburization than the 190 keV Ti-implantation itself; but the dual implant had more Ti, more C, and a greater C/Ti ratio than the low energy Ti implant. We concluded that the improved tribological surface of Ti-implanted steel results from vacuum carburization and not just the presence of excess C.

Ion implantation of metals is moving out of the laboratory and into practice as a surface processing technique for improving the wear life of engineering components. While much emphasis has been placed on N-implantation for improving knives, dies and punches subjected to mild abrasive and adhesive wear environments (1-3), Ti-implantation is receiving considerable attention in the bearing and tool steel community (4,5) because of its ability to reduce friction and wear on hardenable steels subjected to severe wear conditions (6-9).

The improved tribological properties of Ti-implanted steels have been attributed to a unique surface alloy produced by high fluence Ti implantation. The alloy is a mixture of Fe-Ti-C (6-10) with a microstructure shown to be amorphous (8,10). The carbon (C), found in excessively high concentrations near the surface, enters the solid from the vacuum chamber, by a process which can be described as implant-assisted vacuum carburization (8,11). During implantation, sputtering erodes the surface and uncovers implanted Ti, which reacts with residual gases in the vacuum chamber, producing surface carbide species. These carbon atoms then migrate inwards, producing the Fe-Ti-C surface alloy. It is not known, however, whether it is the presence of C itself or the process by which C enters the surface that is responsible for creating this remarkable tribological surface. Dual implants of C and Ti have also produced low wear and low friction surfaces (6,12,13).

50 x 10¹⁶ to 10¹⁷ /cm²

The purpose of this study is to investigate two different ion implantation processes which increase the carbon concentration in Ti-implanted steels. Dry sliding friction and wear measurements were used to evaluate the processes and compare them to the original high fluence ($50 \times 10^{16} / \text{cm}^2$) high energy (190 keV) process. In one process, separate implantations of Ti and C were performed at energies resulting in similar depth distribution for Ti (190 keV) and C (50 keV) atoms. In the second, Ti was implanted at an energy considerably lower (50 keV) than used previously (190 keV). A recent study of the energy dependence of the Ti implantation process (11) has shown that at lower energies, vacuum carburization is initiated sooner and a more fully carburized layer is produced at a lower fluence. Compositions of surfaces implanted with Ti ions to a fluence of $2 \times 10^{17} / \text{cm}^2$ will be presented in order to illustrate the effects of the processing methods on the Ti and C distributions.

2 x 10¹⁷ /cm²

Steel disks were metallographically polished, then implanted with Ti, Ti and C, or C ions. The disks were carefully heat sunk to prevent heating by the ion beam during implantation ($T_{\text{Max}} < 50^{\circ}\text{C}$). Ti ions were implanted to fluences from 5 to $50 \times 10^{16}/\text{cm}^2$ at 50 keV or 190 keV, and C ions to $20 \times 10^{16}/\text{cm}^2$ at 50 keV.

Kinetic friction coefficients (μ_k) were measured under rather severe sliding conditions: low speed (0.1 mm/sec), dry sliding contact in air. The geometry was a 1.27 mm diameter ball sliding against an implanted disk flat (both AISI 52100 steel of hardness $R_C \sim 60$). The ball was loaded to 9.8 N (1 kgf), and up to 20 unidirectional passes were made over the same track. The severity of wear produced during sliding was evaluated by optical (differential interference contrast and interferometry) and electron microscopies.

Table 1 summarizes the friction and wear results for the three implantation processing treatments. Low friction ($\mu \sim 0.3$) values required fluences of $50 \times 10^{16}/\text{cm}^2$, except for the low energy (50 keV) implantation process, which gave $\mu_k = 0.3$ for a fluence of $20 \times 10^{16}/\text{cm}^2$. In each of these four low friction surfaces, damage to the "wear" track was negligible. Debris and/or severe wear (>50 nm) was observed on all other tracks (14) except for the Ti+C implant at $20 \times 10^{16}/\text{cm}^2$, whose track had a smeared layer but only mild (~ 20 nm) wear. This dual implanted surface displayed stick-slip in its friction ($\Delta\mu_k \pm 0.1$); moreover, similar friction and wear behavior resulted when the order of implantation was reversed (i.e. C first, then Ti). By way of comparison, nonimplanted and C (alone) implanted disks had high μ_k max values, 0.6 and 0.7, respectively, and severely damaged wear tracks. Thus, while C implantation somewhat improved the friction and wear behavior of the Ti implanted to $20 \times 10^{16}/\text{cm}^2$ at 190 keV, the low energy implant at the same fluence produced a surface as good as the 190 keV Ti implant (with or without C) at $50 \times 10^{16}/\text{cm}^2$.

The effects of the three processing treatments on the composition of the implanted surface are revealed in composition vs. depth profiles of the three disks implanted with Ti to $20 \times 10^{16} / \text{cm}^2$ (i.e. those of column 2 of Table 1). Composition vs. depth profiles were obtained by Auger spectroscopy with ion milling and interferometry; quantitative analysis of Auger data is based on reference compounds (6,8). Figure 1 presents profiles of Ti and excess C (the 4 at.% of C found in the bulk alloy has been subtracted out). The high-energy implant (disk 1) in Figure 1(a) shows a Ti profile which peaks at about 60 nm and a vacuum carburized layer about 50 nm deep. The non-Gaussian shape of the Ti profile indicates that the surface was sputtered during implantation (15). The dual implant (disk 2) in Figure 1(b) shows a similar Ti profile with implanted C and Ti overlapping one-to-one. (The concentration of Ti in disk 2 is about 20% less than in disk 1 because implanted C dilutes the Fe-Ti alloy.) The low-energy implant (disk 3) in Figure 1(c) also shows a sputtered Ti profile, peaked nearer the surface, and a more fully carburized layer than the high-energy implant, disk 1.

The composition profiles shown in Figure 1 are readily explained in terms of implanted ion ranges (16), sputtering (15) and vacuum carburization (11) effects. At low energies, the Ti range profile is shallower and the peak concentration is larger than at high energies. At a fluence of $20 \times 10^{16} / \text{cm}^2$, more of the shallow, low-energy Ti implants were removed than the more deeply penetrating high-energy Ti implants by sputtering during the implantation process. (The sputtering rate of steel should be nearly the same at energies of 50 keV and 190 keV (17).) However, carburization occurred sooner with the 50 keV Ti implantation because the Ti atoms reached the surface sooner. Thus, in the low-energy Ti implant, we observed less Ti, a shallower Ti distribution with a higher peak concentration, and a more concentrated carburized layer.

Energy dispersive X-ray analysis (EDX) of Ti in the three disks, presented in Table 2, confirmed that a smaller percentage of Ti was retained by the low-energy implant (disk 3) than in the high-energy implants, disks 2 and 1. Retained Ti doses were also determined by graphical integration of Figure 1 and agree to 15% with the EDX values in Table 2. Doses of incorporated C were also obtained by graphical integration. The C to Ti dose ratios for the three disks are listed in Table 2. It is clear from Figure 1 and Table 2 that the low-energy implant (disk 3) was more carburized than the high-energy implant (disk 1), but had less C, less Ti and smaller C/Ti ratio than the dual implant (disk 2). The low-energy implant also had a larger peak concentration than the high-energy implant (32 at.% vs. 22 at.%); however, previous studies have indicated that Ti without sufficient C has a deleterious effect on friction and wear (8,14). We therefore believe that the larger peak Ti concentration obtained by low energy implantation did not play a significant role in the friction behavior; this, however, needs further investigation.

In summary we have evaluated two ion implantation processes which increase the C concentration in Ti-implanted layers above that of the original treatment. Dry sliding friction and wear studies have demonstrated that a low-energy (50 keV) Ti implant can produce a superior tribological surface than a dual implant (Ti at 190 keV plus C at 50 keV) at a lower fluence. A comparison of the compositions of the implanted layers showed that a 50 keV-implanted surface had a more fully carburized layer than a 190 keV-Ti implanted surface, but less C, less retained Ti, and a smaller C to Ti ratio. It thus appears that the C concentration alone is not a controlling factor in the tribological behavior of the Fe-Ti-C layer. More likely, it is the Fe-Ti-C layer produced during the vacuum carburization process which imparts the tribological improvement.

In conclusion, we have found that a vacuum carburized layer is more effective than implanted carbon in forming a superior tribological surface Ti-implanted steel. The fluence required to produce a fully carburized layer decreases as the energy of the implanted Ti decreases. This result is of great practical importance for the ion implantation processing of materials: lower fluences reduce production time and lower energies cut down beam heating problems. It also suggests that if sequential implants are to be performed at several energies (13), e.g. to produce more uniform composition vs. depth profile, that the lowest energy implants should be done first. Dual implants of C and Ti had a somewhat beneficial effect in a bearing steel. We suggest they may prove even more valuable in softer steels where friction reduction by the Ti-induced carburized layer and solid solution strengthening by the C might combine to improve tribological behavior.

Table 1. Maximum Friction Coefficients and Wear Track Damage
 (n-none; m-mild; s-severe) for Three Ti-Implantation
 Processes as a Function of Ion Energy and Fluence.

Process	Energy (kev)	Fluence ($\times 10^{16}/\text{cm}^2$)		
		5	20	:
Low-Energy Ti	50	0.6/s	0.3/n	0.3/n
High-Energy Ti	190	0.8/s	0.8/s	0.3/n
Dual Implant: Ti	190	0.7/s	0.5/m	0.3/n
C	50			

Table 2. Retained Ti Dose and C/Ti Ratio for Three Disks
 Implanted to $2 \times 10^{17} / \text{cm}^2$.

	High-Energy Ti <u>Disk 1</u>	Dual Implant <u>Disk 2</u>	Low-Energy Ti <u>Disk 3</u>
Retained Ti ($\pm 1 \times 10^{16} / \text{cm}^2$) ^a	13	13	9
C/Ti Ratio	0.060	1.0	0.23

a. By EDX, calibrated against a Ti-implanted steel ($5 \times 10^{16} \text{ Ti/cm}^2$ at 190 keV) for which the retention was observed to be almost 100%.

CONCENTRATION PROFILES OF STEEL IMPLANTED TO $2 \times 10^{17}/\text{cm}^2$

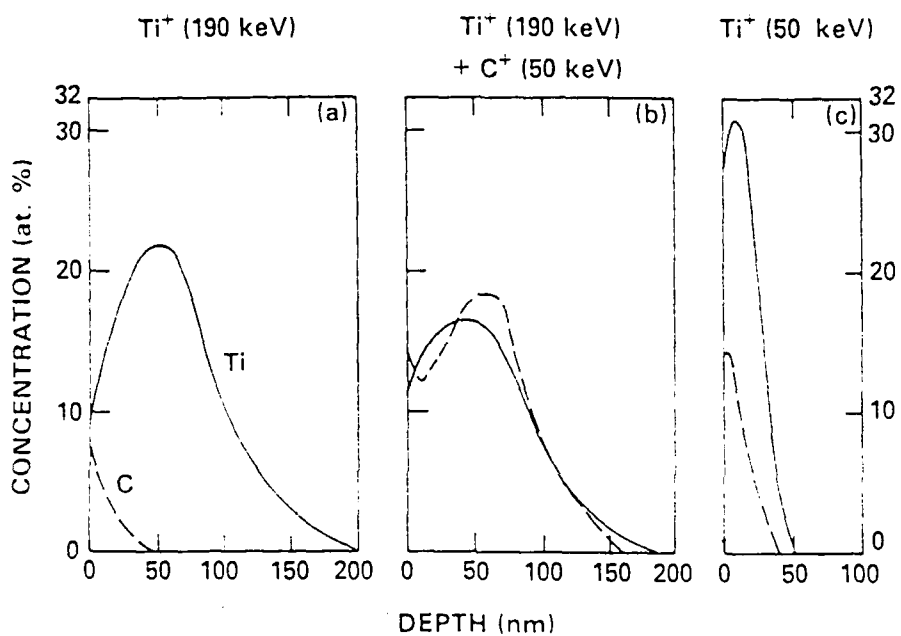


Figure 1. Auger composition vs. depth profiles of Ti and excess C (i.e. above bulk 4 at.%) in 52100 steel implanted to a fluence of $2 \times 10^{17}/\text{cm}^2$ with (a) disk 1: Ti^+ (190 keV); (b) disk 2: Ti^+ (190 keV) + C^+ (50 keV); (c) disk 3: Ti^+ (50 keV).

REFERENCES

1. G. Dearnaley, *J. of Metals*, 34, 18 (1982).
2. G. Dearnaley, *Rad. Effects*, 63, 1 (1982).
3. R.E. Fromson and R. Kossowsky, Metastable Materials Formation by Ion Implantation (S.T. Picraux and W.J. Choyke, editors), Elsevier, Amsterdam, 1982, p. 355.
4. F.A. Smidt, J.K. Hirvonen, and S. Ramalingham, NRL Memorandum Report Number 4616, September 25, 1981.
5. Piran Sioshansi (Spire Corporation, Bedford, Massachusetts), reported at Metallurgical Coatings Conference, San Diego, California, April 1983.
6. C.A. Carosella, I.L. Singer, R.C. Bowers, and C.R. Gossett, Ion Implantation Metallurgy (C.M. Preece and J.K. Hirvonen, editors), Metallurgical Society of AIME, Warrendale, Pennsylvania, 1980, p. 103.
7. I.L. Singer, R.N. Bolster, and C.A. Carosella, *Thin Solid Films*, 73, 283 (1980).
8. I.L. Singer, C.A. Carosella, and J.R. Reed, *Nucl. Inst. and Meth.*, 182/183, 923 (1981).
9. T.E. Fischer, M.J. Luton, J. M. Williams, C.W. White, and B.R. Appleton, ASME/ASLE Lubrication Conference, Washington, D.C., October 1982, ASLE Preprint Number 82-LC-3D-3.
10. J.A. Knapp, D.M. Follstaedt, and S.T. Picraux (C.M. Preece and J.K. Hirvonen, editors), Metallurgical Society of AIME, Warrendale, Pennsylvania, 1980, p. 152; *Appl. Phys. Lett.*, 37, 330 (1980).
11. I.L. Singer, *J. Vac. Sci. Technol.*, A1, 419 (1983).

12. J.K. Hirvonen, C.A. Carosella, R.A. Kant, I.L. Singer, R. Vardiman, and B.B. Rath, *Thin Solid Films*, 63, 5 (1979).
13. F.G. Yost, L.E. Pope, D.M. Follstaedt, J.A. Knapp, and S.T. Picraux, Metastable Materials Formation by Ion Implantation (S.T. Picraux and W.J. Choyke, editors), Elsevier, Amsterdam, 1982, p. 261.
14. A detailed study of the friction and wear behavior of 190 keV Ti implants is reported in I.L. Singer and R.A. Jeffries, *J. Vac. Sci. Technol.*, A1, 317 (1983).
15. F. Schulz and K. Wittmaack, *Rad. Effects*, 29, 31 (1976).
16. P.D. Townsend, J.C. Kelly, and N.E.W. Hartley, Ion Implantation, Sputtering and their Applications, Academic Press, New York, 1976, Chapters 2 and 6.
17. The sputtering yield of steel by Ti ions with energies 25 keV to 200 keV should be constant $S=2.5\pm 0.5$ if one can extrapolate the yield of Ti from Ar. See H.H. Anderson and H.L. Bay in Sputtering by Particle Bombardment I (R. Behrisch, editor), Springer-Verlag, Berlin, 1981, p. 173.

GEO-CENTERS, INC.
ANALYSIS OF CONTRACT REVENUES
FISCAL YEARS 1980, 1981, & 1982

PROJECT NO.	AGENCY	YEAR		
		1980	1981	1982
121	NSWC	\$531		
138	ARRADCOM	\$409		
140	DNA	\$-322		
141	DNA	\$8958		
144	CGA	\$-69		
147	UCOM/DCE	\$10142	\$112	
149	USGS	\$788		
152	ARRADCOM	\$45065		
153	ARRADCOM	\$6136		
158	IRFA	\$51394	\$137349	\$315525
162	INEL	\$27876	\$55931	
163	EGG	\$416		
164	NOSC	\$44926	\$43251	
165	OPR	\$47086	\$32796	\$1561
166	NRC	\$11776		
167		\$-28858		
168	DOE	170358 \$77534	\$490228	\$94808 662570
169	INEL	\$73431	\$-116	
171	NRC	67158 \$8857	\$83431	\$13497
173	NESEC/DSE	\$13112	\$13112	
176	USGS	\$17694	\$63574	
180	NRL	\$11016	\$114797	\$143428
182	NRL	\$44770	\$85938	\$48088
183	ARRADCOM		\$3089	\$77394
184	NRL	\$24601	\$62084	\$8104
185	Patrol Activities NRC	\$28066		
187	ARRADCOM	\$495	\$9413	\$75676
188	INEL	\$16002	\$134044	
192	TMI	\$37355		
193	NESEC	\$9988	\$2231	
195	TMI	\$4450	\$-5	
200	EGG	\$5046	\$19143	
201	TMI	\$3494		
202	ERT - Pacific Island	\$23238	\$8608	
204			\$18265	
209	DEL/DOD		\$8432	\$89405
212	INEL	\$3089		
217	Sea View		\$19246	
218	SEA		\$4851	
219	NOS		\$22045	\$1851
220			\$45430	\$67193
224				\$42840
225	NAF/Edg		\$31596	
228	EGG		\$34960	
229			\$48048	\$41517
230	EGG		\$14806	
232	EGG		\$5072	
235	INEL		\$2000	
242	DMM		\$1972	\$36646
244	NRL		\$8486	\$514
246	America Island		\$21825	

END

DATE
FILMED

9-83

DTI